HHS Public Access

Author manuscript

J Am Chem Soc. Author manuscript; available in PMC 2022 June 20.

Published in final edited form as:

J Am Chem Soc. 2013 March 06; 135(9): 3592–3598. doi:10.1021/ja3119527.

Chiral Sum Frequency Generation for *In Situ* Probing Proton Exchange in Antiparallel β-Sheets at Interfaces

Li Fu[†],

Dequan Xiao[†],

Zhuguang Wang,

Victor S. Batista[*],

Elsa C. Y. Yan[*]

Department of Chemistry, Yale University, 225 Prospect Street, New Haven, CT 06520

Abstract

Studying hydrogen/deuterium (H/D) exchange in proteins can provide valuable insight on protein structure and dynamics. Several techniques are available for probing H/D exchange in the bulk solution, including NMR, mass spectroscopy and Fourier transform infrared spectroscopy. However, probing H/D exchange at interfaces is challenging since it requires surface-selective methods. Here, we introduce the combination of *in situ* chiral sum frequency generation (cSFG) spectroscopy and *ab initio* simulations of cSFG spectra as a powerful methodology to probe the dynamics of H/D exchange at interfaces. This method is applied to characterize H/D exchange in the antiparallel β-sheet peptide $LK_7β$. We report here for the first time that the rate of D-to-H exchange is about one order of magnitude faster than H-to-D exchange in the anti-parallel structure at the air/water interface, which is consistent with the existing knowledge that O-H/D dissociation in water is the rate limiting step, and breaking the O-D bond is slower than breaking the O-H bond. The reported analysis also provides fundamental understanding of several vibrational modes and their couplings in peptide backbones that have been difficult to characterize by conventional methods, including Fermi resonances of various combinations of peptide vibrational modes such as amide I and amide II, C-N stretch, and N-H/N-D bending. These results demonstrate cSFG as a sensitive technique for probing the kinetics of H/D exchange in proteins at interfaces, with high signal-to-noise N-H/N-D stretch bands that are free of background from the water O-H/O-D stretch.

Graphical Abstract

[*]Corresponding authors: elsa.yan@yale.edu, victor.batista@yale.edu.
[†]Equal Contribution

Supporting Information Available: Description of the material and method, spectral analysis and *ab initio* calculation, and supplementary figures included. This material is available free of charge via the Internet at http://pubs.acs.org.

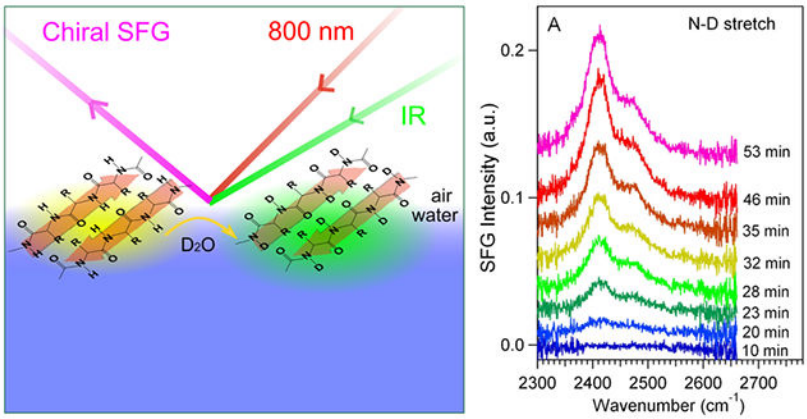

Introduction

Probing hydrogen/deuterium (H/D) exchange in proteins in bulk solutions has proven very useful to reveal protein dynamics and structures.[1] NMR,[2] mass spectrometry (MS)[3] and Fourier transform infrared spectroscopy (FTIR)[4] have been used to probe H/D exchange in protein to yield information about structures of intermediates of protein folding,[5,6] kinetics and structures of amyloid aggregation,[7–11] and conformational changes of proteins upon ligand binding.[12–14] Nonetheless, there is a lack of surface-selective methods that allow real-time and *in situ* characterization of H/D exchange in proteins at interfaces. Such characterization is expected to be useful to reveal interactions among proteins, water, and biomembranes, enabling investigations, such as solvent accessibility of proteins embedded in membranes, proton transfer[15] and intramolecular hydrogen-bonding interactions[16] in membrane proteins, and water channels formed by transmembrane proteins.[17,18]

Although the peptide N-H/N-D stretch can directly reveal proton exchange in proteins, characterization of the N-H/N-D stretch of proteins in aqueous environments using conventional vibrational methods has remained challenging. The challenge comes from the overwhelming O-H/O-D stretch of water background that overlaps with the N-H/N-D stretch. We recently demonstrated that chiral sum frequency generation (cSFG) spectroscopy can probe peptide N-H stretch with zero water background.[19] On the basis of this finding, we introduce cSFG as a method for *in situ* probing H/D exchange in proteins at interfaces in real time.

Both experimental approaches[19–24] and theory[25–30] of sum frequency generation spectroscopy have been evolving in a fast pace. These developments have served as a basis to establish cSFG as a biophysical analytical tool to characterize biointerfaces.[31] It has been applied to study various biomolecules, including DNA[32,33] and proteins.[19,24,31] Recently, we found that cSFG can provide a set of vibrational optical signatures for characterizing protein secondary structures at interfaces,[19,31] similar to the use of circular dichroism (CD) spectroscopy to characterize protein secondary structures in bulk solution. The N-H stretch along the peptide backbones at ~3300 cm^{-1} probed by cSFG is characteristic to β-sheet and α-helical structures at interfaces.[31] Using this chiral N-H stretch together with the chiral amide I signal, we studied the misfolding of human islet amyloid polypeptide (hIAPP),

an amyloid protein associated with type II diabetes, upon interactions with a lipid/water interface. We observed the misfolding of hIAPP from disordered structures to α-helical structures and then to β-sheet structures *in situ* and in real time.

In this study, we used the $LK_7β$ peptide, which has a sequence of LKLKLKL.[34] This peptide forms an antiparallel β-sheet at amphiphilic interfaces. It has been extensively characterized by a wide range of methods, including CD,[34] FTIR,[34] and conventional (achiral) SFG.[35–37] Chen and coworkers probed antiparallel β-sheets using cSFG, focusing on the amide I vibrational modes. They observed a strong amide I signal.[24] In general, antiparallel β-sheets adopt D_2 symmetry, which is proposed to give strong non-linear optical response.[38,39] Indeed, when we used cSFG to characterize the structure of $LK_7β$ at the air/water interface in this study, we observed that $LK_7β$ at the air/water interface exhibits strong cSFG signals of peptide backbone in both N-H/N-D stretch and amide I regions. Using the N-H/N-D stretch signals, we monitor the H/D exchange of $LK_7β$ at the air/water interface upon H_2O/D_2O solvent exchange *in situ* and in real time.

Our cSFG spectra of $LK_7β$ in the N-H and N-D stretch regions exhibit subtle vibrational features, which have not been observed by conventional vibrational spectroscopies due to the overwhelming O-H/O-D stretch water background. In order to analyze these spectral features, we performed *ab initio* SFG simulation and normal mode analysis to explore various possibilities of assigning these vibrational features, which include amide I/amide II combinational band, amide I and amide II overtones, free N-H group exposed to the solvent environment, and C-N stretch/N-D bending combinational band. Understanding these vibrational features can reveal coupling of various vibrational modes along peptide backbones, which is fundamentally important for investigations of vibrational energy redistribution in proteins in aqueous environments.

Experimental Section

cSFG Experiments.

We obtained the cSFG spectra of $LK_7β$ peptide at the air/water interface using our broadband SFG spectrometer,[40] which is described in Ma *et al.* and the Supporting Information. In this study, the *psp* polarization setting (*p*-polarized SFG, *s*-polarized visible, and *p*-polarized IR) was used for cSFG detection. We first obtained the chiral amide I spectra, and then N-H and N-D spectra using H_2O and D_2O as the solvent, respectively. To probe the H-to-D exchange, we added D_2O into the H_2O solution of $LK_7β$ to initiate the exchange process and then monitor the N-D stretch spectra. In the experiments, we used a final ratio of D_2O: H_2O equal to 1:4 (1.00 mL D_2O into 4.00 mL H_2O) or 1:2 (1.67 mL D_2O into 3.33 mL H_2O). Similarly, to probe the D-to-H exchange, we added H_2O into the D_2O solution of $LK_7β$ and then monitored the N-H stretch spectra. D_2O or H_2O was added along the side of the Teflon beaker without additional stirring to avoid surface perturbation.

Materials and Data Acquisition.

The $LK_7β$ peptide were synthesized and purified by the W.M. Keck Biotechnology Resource Laboratory at Yale University. The lyophilized $LK_7β$ peptide was dissolved in deionized

water and distributed into vials, which was frozen in liquid nitrogen and stored at −80°C. Each vial of the solution was thawed for one SFG experiment and never frozen again. In the SFG experiments, a Teflon beaker containing phosphate buffer (10 mM phosphate, pH/pD=7.4) was placed on the sample stage. The pD values were obtained using a correction of pD = pH + 0.4.[41,42] A stock solution of $LK_7\beta$ was added using a micro-syringe to give a final concentration of 25 μM. The H/D exchange was initiated by adding D_2O into H_2O, or adding H_2O into D_2O. While each cSFG spectrum in the kinetic studies was taken with an acquisition time of 1 min, other spectra were taken with an acquisition time of 10 min. The raw spectra were processed by the steps of removing the contribution from cosmic rays, subtracting background, calibrating the wavenumber, and normalizing to the IR power, as previously desecribed.[40] The processed spectra were then fitted into the following equation.

$$I_{SFG} \propto \left| \chi_{NR}^{(2)} + \sum_q \frac{A_q}{\omega_{IR} - \omega_q + i\Gamma} \right|^2 \quad (1),$$

where I_{SFG} is the sum frequency generation intensity, χ_{NR} is the nonresonant second-order susceptibility, ω_{IR} is the input IR frequency, and A_q, ω_q, and Γ_q are the amplitude, resonant frequency, and damping factor of the q^{th} vibration mode, respectively.

Ab initio Simulation of SFG Spectra.

We built an antiparallel β-sheet model using two peptides. Each contains four glycine residues and two cysteine residues. The two peptides are linked to each other in an antiparallel configuration by two disulfide bonds at the ends of the peptides (Scheme 1), forming an anti-parallel β-sheet. The Gaussian 09 program[43] was used to perform geometry optimization and normal mode analysis at the density functional theory (DFT) level for the anti-parallel β-sheet, using the B3LYP functional and the 6-31G* basis set. With the same DFT method and basis set, the dipole derivatives $\partial\mu_n/\partial Q_q$ and polarizability derivatives $\partial\alpha_{lm}/\partial Q_q$ (where n, l, m are the indexes of directions in the Cartesian coordinate, and Q denotes for the normal mode coordinate) for the q^{th} normal mode were computed using the keywords ‘iop(7/33=1)’ and ‘polar’, respectively. The computed $\partial\mu_n/\partial Q_q$ and $\partial\alpha_{lm}/\partial Q_q$ yield the vibrational hyperpolarizability tensors through $\beta_{lmn,q} \propto \frac{\partial\alpha_{lm}}{\partial Q_q}\frac{\partial\mu_n}{\partial Q_q}$. Finally, we computed the 2nd-order susceptibility tensor elements using Euler transformation, and simulated the *psp* cSFG spectra as described in our previous work.[44] To compare the calculated SFG spectra with the experiment spectra, the calculated vibrational frequencies of all of the normal modes in this study were scaled using a common factor of 0.9322.

Results

In this section, we will first present the cSFG spectra of $LK_7\beta$ at the air/water interface in the amide I region, and then the N-H and N-D stretch regions using H_2O and D_2O as solvent, respectively. Subsequently, we will show how cSFG can be used to monitor the kinetics of H/D exchange in $LK_7\beta$ at the air/water interface using the chiral N-D and N-H stretch vibrational modes. Finally, we report the results of *ab initio* calculations and peak assignments in the N-H and N-D stretch spectra of $LK_7\beta$.

Amide I Spectra at the Air/Water Interfaces.

We obtained the cSFG spectrum of $LK_7\beta$ at the air/H_2O interface in the amide I region. The spectrum shows a peak at 1619 cm^{-1} and a shoulder at 1690 cm^{-1} (Figure 1), which are the characteristic B_2 mode and B_1 mode of the amide I vibrations of antiparallel β-sheets, respectively.[24] These peak positions agree with previous characterizations using FTIR and polarized modulated infrared reflection-adsorption spectroscopy (IRRAS) methods.[45,46] We also obtained the chiral amide I spectrum of $LK_7\beta$ at the air/D_2O interface and observed that the B_2 band shifts from 1619 cm^{-1} to 1616 cm^{-1} (Figure 1). This kind of red shift in the amide I band is commonly observed in various protein secondary structures due to the isotope shift of the N-H/N-D in-plane bending mode that contributes to the amide I band.[47,48] The B_1 band in the D_2O spectrum becomes less obvious (Figure 1, inset). The observation of the characteristic B_2 mode (1620 cm^{-1}) and B_1 mode (1690 cm^{-1}) of the amide I vibrations at the air/H_2O interface indicates that $LK_7\beta$ forms antiparallel β-sheet structures.

N-H/N-D Stretch Spectra at the Air/Water Interfaces.

We obtained the N-H and N-D stretch spectra of $LK_7\beta$ at the air/H_2O and air/D_2O interfaces, respectively (Figure 2). These spectra were fitted into Eq. 1, and the fitting parameters are summarized in Table 1. The fitting results show that the N-H spectrum exhibits a peak at 3268 cm^{-1} and a shoulder at 3178 cm^{-1}, while the N-D spectrum displays a peak at ~2410 cm^{-1} and a shoulder at ~2470 cm^{-1}. We will discuss the assignments of these vibrational bands in the *Spectral Analysis* section.

H/D Exchange of $LK_7\beta$ at the Air/Water Interfaces.

We used the chiral N-D and N-H stretch signals (Figure 2) to monitor the kinetics of proton exchange in $LK_7\beta$ at interfaces. We initiated the H/D exchange process upon addition of D_2O into the H_2O solution of $LK_7\beta$ or addition of H_2O into the D_2O solution of $LK_7\beta$. Figure 3 shows the time-dependent cSFG spectra of $LK_7\beta$ in the N-D and N-H stretch regions. Figures 3A and 3B present the kinetics of H-to-D exchange (addition of D_2O to H_2O) with a final H_2O:D_2O ratios of 4:1 and 2:1, respectively. The N-D signals gradually build up in the spectra. Similarly, Figures 3C and 3D present the kinetics of D-to-H exchange (addition of H_2O to D_2O) with a final H_2O:D_2O ratios of 1:4 and 1:2, respectively. The N-H signals gradually increase upon addition of H_2O. These results demonstrate the *in situ* and real-time kinetics of the proton exchange along the peptide backbone of $LK_7\beta$ at the air/water interface.

Figure 3 shows that the rates of H-to-D and D-to-H exchange are different. For the systems with a ratio of 4:1 (D_2O:H_2O or H_2O:D_2O), the H-to-D exchange (Figure 3A) takes ~50 minutes to complete while the D-to-H exchange (Figure 3C) takes ~10 min. Similarly, for the systems with a ratio of 2:1 (D_2O:H_2O or H_2O:D_2O), the H-to-D exchange (Figure 3B) takes ~30 minutes while the D-to-H exchange (Figure 3D) takes ~5 min. Figure 4 shows the plots of SFG field for the N-H (3268 cm^{-1}) and N-D (2410 cm^{-1}) stretch as a function of time. The plots can be fitted into a stretched exponential function (Supporting Information), which reveal the empirical relaxation of the D-to-H exchange in one order of magnitude faster than that of the H-to-D exchange. We realize that this empirical comparison is

qualitative; however, a quantitative comparison requires a development and validation of a kinetic model, which is out of the scope of our current study that is to develop cSFG as a new method for probing real-time kinetics of proton exchange in proteins at aqueous interfaces.

Spectral Analyses and Ab Initio SFG Simulations.

We performed *ab initio* SFG simulation and normal mode analysis to reveal the origin of experimentally observed chiral N-H and N-D stretch vibrational bands in Figure 2, where the N-H spectrum (Figure 2A) shows a major peak at 3268 cm^{-1} and a shoulder at 3178 cm^{-1}, while the N-D spectrum (Figure 2B) shows a major peak at 2410 cm^{-1} and a shoulder at 2470 cm^{-1}.

We started by assigning the major peaks in the cSFG spectra of $LK_7\beta$ (Figure 2). We ascribe the major peaks at 3268 cm^{-1} (Figure 2A) and 2410 cm^{-1} (Figure 2B) to the N-H and N-D stretches of the peptide backbone, respectively. These assignments are consistent with Rozenberg and Shoham's assignment for non-deuterated and deuterated antiparallel β-sheets.[49] They used FTIR to study antiparallel β-sheets formed by poly-lysines and found that the N-H stretch frequency is at 3270 cm^{-1}, while the N-D stretch frequency is shifted to 2410 cm^{-1}. Moreover, we performed *ab initio* calculations to simulate the cSFG spectra (Figure 5). The normal mode analysis suggests that N-H and N-D stretches of the anti-parallel β-sheets are both IR and Raman active, rendering SFG activity. Using a common scaling factor of 0.9322, the major peak in the N-H spectrum appears at 3268 cm^{-1} (Figure 5A), while the major peak in the N-D spectrum appears at 2405 cm^{-1} (Figure 5B). This relative positioning of major peaks between the N-H and N-D stretches agree with our experimental results (Figure 2).

Besides the major peaks, the cSFG spectra also show shoulder peaks at ~3178 cm^{-1} in the N-H spectrum (Figure 2A) and ~2470 cm^{-1} in the N-D spectrum (Figure 2B). Since, these spectral features have never been reported previously, we assigned these peaks based on the normal mode analysis from *ab initio* calculations and additional chiral SFG experiments. We explored the following possibilities for the assignments: (i) amide II overtone, (ii) amide I overtone, and (iii) N-H stretch of free N-H groups (*i.e.*, the N-H groups exposed to the solvent). However, the results of our calculations and additional control experiments prompt us to eliminate these possibilities based on unmatched calculated frequencies, which are discussed in the Supporting Information. Subsequently, we tentatively assign the 3178-cm^{-1} shoulder peak to the Fermi resonance of the combinational band of the amide I and amide II modes with the N-H stretch, and the 2470-cm^{-1} shoulder peak to the Fermi resonance of the combination band of the C-N stretch and the N-D in-plane bending with the N-D stretch (Table 2). Below, we elucidate the rationale for these assignments.

First, we discuss the 3178-cm^{-1} shoulder peak in the N-H spectrum (Figure 2A). According to previous studies, the ~3178-cm^{-1} peak can possibly be due to the Fermi resonance of the combinational mode of amide I and amide II.[50] To test this possibility, we performed normal mode analyses in the N-H stretch regions of the antiparallel β-sheet model (Scheme 1). The computed vibrational frequency is 1626 cm^{-1} for amide I and 1545 cm^{-1} for amide II. The combination band should have a frequency of ~3171 cm^{-1}, which is close to the

experimental value (3178 cm^{-1}). To confirm this assignment, we further obtained the amide II spectrum of $LK_7\beta$ (Figure S1), which shows an amide II band at 1563 cm^{-1}. Since the amide I band is at 1619 cm^{-1} (Figure 1), the combination band of amide I and amide II is at 3182 cm^{-1}, which is close to 3178 cm^{-1}. Hence, we attribute the shoulder peak at 3178 cm^{-1} (Figure 2A) to the Fermi resonance of a combination band due to amide I and amide II with N-H stretch.

Then, we discuss the assignment of the 2473-cm^{-1} shoulder peak (Figure 2B). The peak can possibly be due to the Fermi resonance of a combinational band of C-N stretch and N-D in-plane bending with the N-D stretch, as suggested by Krimm and coworkers.[51,52] We performed *ab initio* calculations to examine this assignment. Our calculation shows that the C-N stretch is at 1422 cm^{-1} and the N-D in-plane bending is at 1044 cm^{-1}. Hence, the combination band is at 2466 cm^{-1}, which is close to the experimental value of 2473 cm^{-1}. To further test this assignment, we obtained the cSFG spectra of $LK_7\beta$ in the C-N stretch region (Figure S1) and observed a vibrational band at ~1470 cm^{-1}. This frequency is deviated from the calculated value (1422 cm^{-1}). The red-shift of the calculated C-N stretch (amide II') frequency could be attributed to the lack of explicit solvent interactions between amide groups and water as discussed in the literature.[53] We also attempted to experimentally obtain cSFG spectrum of $LK_7\beta$ in the N-D bending region (~1000 cm^{-1}). Nonetheless, we were not able to observe the N-D bending band, which is perhaps due to our experimental limit of the lower IR energy in the 1000-cm^{-1} region, and/or the weak chiral SFG signal of the N-D bending mode as shown by the *ab initio* SFG simulations (Supporting Information). We also explored other possibilities of assigning the 2473-cm^{-1} peak, including the overtone of amide II'. Nonetheless, we eliminated these possibilities due to the poor agreement between the calculated and experimental frequencies (see the Supporting Information). Therefore, we ascribed the appearance of the 2473-cm^{-1} shoulder peak to the Fermi resonance of the combination band of C-N stretch and N-D in-plane bending with the N-D stretch.

Discussion

Summary.

We have used cSFG to monitor the N-H/N-D signals of the peptide backbone upon H_2O/D_2O solvent exchange and observed an *in situ* H/D exchange in $LK_7\beta$ at the air/water interface. We found that the rate of D-to-H exchange is faster than that of H-to-D exchange. Because cSFG is free of the background of water O-H stretches, we have observed subtle vibrational feature that were difficult to observe using conventional vibrational methods. We found both the N-H and N-D spectra show a major peak and a shoulder. The N-H spectrum exhibits a major peak at 3268 cm^{-1} and a red-shifted shoulder peak at 3178 cm^{-1}, while the N-D spectrum displays a major peak at 2410 cm^{-1} and a blue-shifted shoulder at 2473 cm^{-1}. We performed *ab initio* normal mode analysis and assigned the shoulder peaks to the Fermi resonance between the N-H stretch and the combination band of amide I and amide II, and the Fermi resonance between the N-D stretch and the combination band of C-N stretch and N-D in-plane bending, respectively.

Differences in the rates of D-to-H and H-to-D exchange.

We observed that the rates of D-to-H exchange are faster than the rates of H-to-D exchange by roughly one order of magnitude. This result suggests that the rate-determining step of the H/D exchange in $LK_7\beta$ at the air/water interface involves breaking the water O-H/O-D bond rather than the N-H/N-D bond of the peptide. Because the zero-point energy of the O-D stretch is lower than that of the O-H stretch, it needs higher energy to break an O-D bond than an O-H bond. For the H-to-D exchange in peptide, the rate-determining step is to break the O-D bond in water; thus, the activation energy is higher and the rate is slower. For the D-to-H exchange in peptide, the rate-determining step is to break the O-H bond in water. Hence, the activation energy is lower and the rate is faster. Ribeiro-Claro *et al.* used Raman spectroscopy to monitor the O-H/O-D stretch of crystalline α-cyclodextrin upon exposure to the H_2O/D_2O vapor. They found that the D-to-H exchange is 7-10 times faster than the H-to-D exchange and concluded that the rate-determining step of the H/D exchange is to break the O-H/O-D bond in water vapour,[54] which aligns with our interpretation. Moreover, Englander and coworkers also measured the H-to-D and D-to-H exchange using NMR for bulk solutions.[42] According to their results, the D-to-H exchange rate constant is about ~5 times faster than that of H-to-D exchange at pH 6, which is also in agreement with our observations of proton exchange at interfaces.

Increases versus decreases in the N-D/N-H stretch signals.

In our experiments, we chose to monitor the increase of the N-D/N-H stretch signals rather than the decrease of the N-D/N-H stretch signals to study the kinetics of proton exchange in $LK_7\beta$ (Figure 2). When we examined the decrease in the N-H (N-D) signals in the H-to-D (D-to-H) exchange process, we indeed observed a substantial decrease of the N-H (N-D) signal towards the end of the exchange process (Figure S3, in the Supporting Information). However, at the beginning of the exchange, we observed fluctuations of the cSFG signal (Figure S4), which could be due to perturbation to the interface upon addition of H_2O/D_2O, and/or nonhomogeneous solution during the acquisition time. Nonetheless, when we monitored the increase of the N-H (N-D) signal in the D-to-H (H-to-D) exchange process, we detected the N-H (N-D) signal accumulating on top of zero background, which allows an observation of a steady increase of the N-H stretch signals that can reveal the kinetics of the exchange process.

N-H stretch in the lysine side chain.

Although it is possible to assign the N-H/D-H stretch to the amine group of the lysine residue in $LK_7\beta$,[55] this assignment does not apply to our observed chiral N-H/N-D stretch signals under our experimental conditions, which is based on three considerations. First, the H/D exchange in charged side chains is known to be instantaneous or diffusion limited,[1] while the H/D exchange on the amide backbone has been previously shown to be on the time scale ranging from minutes to days.[1] Because we observed the exchange rates are on the time scale of minutes in our studies, the chiral N-H signal is not likely due to the lysine residue. Second, the $-NH_3^+$ group has the asymmetric N-H stretch at 3000-3200 cm^{-1} and the symmetric N-H stretch at 2100-2600 cm^{-1}. The cSFG spectrum (Figure 2) shows the chiral N-H stretch at 3300 cm^{-1}, which does not match with the N-H stretch frequencies of

the $-NH_3^+$ group. Moreover, the phosphate buffer in our experiments maintained the bulk pH at 7.4, and the $-NH_3^+$ group of lysine has a pK_a at 10.5. Although the surface pK_a of lysine may change, a previous study performed by the Eisenthal group shows that the pK_a of $CH_3(CH_2)_{21}NH_3^+$ only changes from 10.7 to 9.9 at the air/water interface.[56] Thus, the lysine side chain should remain protonated at the air/water interface. Third, we previously showed that the α-helical $LK_{14}α$ $(LKKLLKL)_2$ also exhibit chiral N-H signals. Since both $LK_{14}α$ and $LK_7β$ contain only the lysine and leucine residues, if our observed chiral N-H stretch is due to the Lys residue, we would expect the N-H stretch frequency of the $LK_{14}α$ and $LK_7β$ peptides to be the same. Nonetheless, the chiral N-H stretch of $LK_{14}α$ is at 3304 cm^{-1}, while that of $LK_7β$ is at 3268 cm^{-1}. We previously attributed this 40-cm^{-1} shift in the chiral N-H stretch frequency to the different hydrogen bonding environments of the peptide N-H group in different protein secondary structures. Based on these considerations, we assign the observed cSFG signals to the peptide backbone N-H stretch.

Sensitivity of cSFG in detecting N-H/N-D stretch in aqueous environments.

Our results demonstrate that cSFG has the selectivity of chirality and interface to probe the N-H/N-D stretch of peptides free of the O-H stretch background of water. Since water molecules do not form chiral structures at interfaces, cSFG is muted to water O-H stretch signals. Thus, cSFG can provide N-H/N-D stretch spectra of proteins at interfaces in a high signal-to-noise level free of water background. Consequently, cSFG can be used to study detailed coupling of various vibrational modes of the peptide backbones in the N-H/N-D regions. These vibrational modes include the amide I, amide II, C-N stretch and their various overtones and combinational modes. Except in the gas phase,[57,58] the studies of vibrational coupling in the N-H/N-D region in aqueous solution have been difficult using conventional vibrational methods because of the overwhelming broad O-H/O-D stretch band of water. Here, our results show that cSFG can tackle this problem, introducing a method for probing vibrational couplings and vibrational energy distribution along peptide backbones.

Conclusion

On the basis of our results, we conclude that cSFG spectroscopy is a label-free, background-free method to study real-time kinetics of proton exchange in proteins *in situ* at interfaces. Using cSFG to monitor the N-H/N-D stretch of the $LK_7β$ peptide backbone, we observed that the rate of D-to-H exchange is about an order of magnitude faster than that of H-to-D exchange in the $LK_7β$ anti-parallel structure at the air/water interface. These results demonstrate that further applications of cSFG in characterizing the peptide N-H/N-D stretch can potentially address a number of important problems related to interactions of proteins with water and membrane. Since protein secondary structures are constructed by the peptide N-H/N-D hydrogen bonding interactions, the hydrogen bonding environments for the peptide N-H/N-D groups are different in different secondary structures. Because cSFG can be used to detect the N-H/N-D stretch frequencies in aqueous environments, cSFG can provide a new tool for characterizing protein secondary structures at interfaces. Moreover, being an optical method, cSFG can be used to characterize the N-H/N-D peptide stretch *in situ* and in real time. Thus, it can provide kinetic information to reveal protein stability and protein folding at interface. We expect that further experimental developments of the

cSFG method can allow investigations of solvent accessibility of proteins embedded in membranes, proton transfer across membrane mediated by proteins, and intermolecular and intramolecular hydrogen bonding interactions in transmembrane proteins.

Supplementary Material

Refer to Web version on PubMed Central for supplementary material.

Acknowledgement

E.Y. is the recipient of the Starter Grant Award, Spectroscopy Society of Pittsburgh. This work is supported by the National Science Foundation (NSF) Grant CHE 1213362. V.S.B. acknowledges supercomputer time from NERSC and support from the National Science Foundation (NSF) Grant CHE 0911520, and the National Institutes of Health (NIH) Grants 1R01 GM-084267-01 and GM-043278 for methods development.

References

(1). Englander SW; Downer NW; Teitelba H Annu. Rev. Biochem 1972, 41, 903–924. [PubMed: 4563445]

(2). Wand AJ; Roder H; Englander SW Biochemistry 1986, 25, 1107–1114. [PubMed: 3008820]

(3). Engen JR Anal. Chem 2009, 81, 7870–7875. [PubMed: 19788312]

(4). Zhang YP; Lewis RNAH; Hodges RS; McElhaney RN Biochemistry 1992, 31, 11572–11578. [PubMed: 1445892]

(5). Englander SW Annu. Rev. Biophys. Biomolec. Struct 2000, 29, 213–238.

(6). Baldwin RL Curr. Opin. Struc. Biol 1993, 3, 84–91.

(7). Tobler SA; Fernandez EJ Protein Sci. 2002, 11, 1340–1352. [PubMed: 12021433]

(8). Kheterpal I; Wetzel R Accounts Chem.Res 2006, 39, 584–593.

(9). Qi W; Zhang A; Patel D; Lee S; Harrington JL; Zhao L; Schaefer D; Good TA; Fernandez EJ Biotechnol. Bioeng 2008, 100, 1214–1227. [PubMed: 18351682]

(10). Wilson LM; Mok Y-F; Binger KJ; Griffin MDW; Mertens HDT; Lin F; Wade JD; Gooley PR; Howlett GJ J. Mol. Biol 2007, 366, 1639–1651. [PubMed: 17217959]

(11). Lu X; Wintrode PL; Surewicz WK Proc. Natl. Acad. Sci. USA 2007, 104, 1510–1515. [PubMed: 17242357]

(12). Busenlehner LS; Armstrong RN Arch. Biochem. Biophys 2005, 433, 34–46. [PubMed: 15581564]

(13). Paterson Y; Englander SW; Roder H Science 1990, 249, 755–759. [PubMed: 1697101]

(14). Powell KD; Ghaemmaghami S; Wang MZ; Ma LY; Oas TG; Fitzgerald MC J. Am. Chem. Soc 2002, 124, 10256–10257. [PubMed: 12197709]

(15). le Coutre J; Gerwert K FEBS Lett. 1996, 398, 333–336. [PubMed: 8977133]

(16). Garczarek F; Gerwert K Nature 2006, 439, 109–112. [PubMed: 16280982]

(17). Murata K; Mitsuoka K; Hirai T; Walz T; Agre P; Heymann JB; Engel A; Fujiyoshi Y Nature 2000, 407, 599–605. [PubMed: 11034202]

(18). Zhu FQ; Tajkhorshid E; Schulten K FEBS Lett. 2001, 504, 212–218. [PubMed: 11532456]

(19). Fu L; Liu J; Yan ECY J. Am. Chem. Soc 2011, 133, 8094–8097. [PubMed: 21534603]

(20). Belkin MA; Han SH; Wei X; Shen YR Phys. Rev. Lett 2001, 87, 113001-1–113001-4. [PubMed: 11531520]

(21). Belkin MA; Kulakov TA; Ernst KH; Yan L; Shen YR Phys. Rev. Lett 2000, 85, 4474–4477. [PubMed: 11082574]

(22). Fu L; Ma G; Yan ECY J. Am. Chem. Soc 2010, 132, 5405–5412. [PubMed: 20337445]

(23). Ji N; Shen YR Chirality 2006, 18, 146–158. [PubMed: 16432921]

(24). Wang J; Chen XY; Clarke ML; Chen Z Proc. Natl. Acad. Sci. USA 2005, 102, 4978–4983. [PubMed: 15793004]

(25). Haupert LM; Simpson GJ Annu. Rev. Phys. Chem 2009, 60, 345–365. [PubMed: 19046125]
(26). Perry JM; Moad AJ; Begue NJ; Wampler RD; Simpson GJ J. Phys. Chem. B 2005, 109, 20009–20026. [PubMed: 16853586]
(27). Simpson GJ J. Chem. Phys 2002, 117, 3398–3410.
(28). Simpson GJ Chemphyschem 2004, 5, 1301–1310. [PubMed: 15499846]
(29). Auer BM; Skinner JL J. Phys. Chem. B 2008, 113, 4125–4130.
(30). Auer BM; Skinner JL Chem. Phys. Lett 2009, 470, 13–20.
(31). Fu L; Wang Z; Yan ECY Int. J. Mol. Sci, 2011, 12, 9404–9425. [PubMed: 22272140]
(32). Walter SR; Geiger FM J. Phys. Chem. Lett 2009, 1, 9–15.
(33). Stokes GY; Gibbs-Davis JM; Boman FC; Stepp BR; Condie AG; Nguyen ST; Geiger FM J. Am. Chem. Soc 2007, 129, 7492–7493. [PubMed: 17521190]
(34). DeGrado WF; Lear JD J. Am. Chem. Soc 1985, 107, 7684–7689.
(35). Weidner T; Apte JS; Gamble LJ; Castner DG Langmuir 2009, 26, 3433–3440.
(36). Weidner T; Breen NF; Li K; Drobny GP; Castner DG Proc. Natl. Acad. Sci. USA 2010, 107, 13288–13293. [PubMed: 20628016]
(37). Mermut O; Phillips DC; York RL; McCrea KR; Ward RS; Somorjai GA J. Am. Chem. Soc 2006, 128, 3598–3607. [PubMed: 16536533]
(38). Ostroverkhov V; Ostroverkhova O; Petschek RG; Singer KD; Sukhomlinova L; Twieg RJ Selected Topics in Quantum Electronics, IEEE Journal of 2001, 7, 781–792.
(39). Ostroverkhov V; Singer KD; Petschek RG J. Opt. Soc. Am. B-Opt. Phys 2001, 18, 1858–1865.
(40). Ma G; Liu J; Fu L; Yan ECY Appl. Spectrosc 2009, 63, 528–537. [PubMed: 19470209]
(41). Glasoe PK; Long FA J. Phys. Chem 1960, 64, 188–190.
(42). Connelly GP; Bai YW; Jeng MF; Englander SW Proteins 1993, 17, 87–92. [PubMed: 8234247]
(43). Frisch MJ; Trucks GW; Schlegel HB; Scuseria GE; Robb MA; Cheeseman JR; Montgomery JA; Vreven T; Kudin KN; Burant JC; Millam JM; Iyengar SS; Tomasi J; Barone V; Mennucci B; Cossi M; Scalmani G; Rega N; Petersson GA; Nakatsuji H; Hada M; Ehara M; Toyota K; Fukuda R; Hasegawa J; Ishida M; Nakajima T; Honda Y; Kitao O; Nakai H; Klene M; Li X; Knox JE; Hratchian HP; Cross JB; Bakken V; Adamo C; Jaramillo J; Gomperts R; Stratmann RE; Yazyev O; Austin AJ; Cammi R; Pomelli C; Ochterski JW; Ayala PY; Morokuma K; Voth GA; Salvador P; Dannenberg JJ; Zakrzewski VG; Dapprich S; Daniels AD; Strain MC; Farkas O; Malick DK; Rabuck AD; Raghavachari K; Foresman JB; Ortiz JV; Cui Q; Baboul AG; Clifford S; Cioslowski J; Stefanov BB; Liu G; Liashenko A; Piskorz P; Komaromi I; Martin RL; Fox DJ; Keith T; Al-Laham MA; Peng CY; Nanayakkara A; Challacombe M; Gill PMW; Johnson B; Chen W; Wong MW; Gonzalez C; Pople JA; Revision C.02 ed; Gaussian, Inc., Wallingford, CT: 2004.
(44). Xiao D; Fu L; Liu J; Batista VS; Yan ECY J. Mol. Biol
(45). Castano S; Desbat B; Dufourcq J BBA - Biomembranes 2000, 1463, 65–80. [PubMed: 10631295]
(46). Buffeteau T; Le Calvez E; Castano S; Desbat B; Blaudez D; Dufourcq JJ Phys. Chem. B 2000, 104, 4537–4544.
(47). Tamm LK; Tatulian SA Q. Rev. Biophys 1997, 30, 365–429. [PubMed: 9634652]
(48). Barth A; Zscherp CQ Rev. Biophys 2002, 35, 369–430.
(49). Rozenberg M; Shoham G Biophys. Chem 2007, 125, 166–171. [PubMed: 16919385]
(50). Lal BB; Nafie LA Biopolymers 1982, 21, 2161–2183. [PubMed: 7171731]
(51). Krimm S; Dwivedi AM J. Raman Spectrosc 1982, 12, 133–137.
(52). Dwivedi AM; Krimm S Biopolymers 1982, 21, 2377–2397.
(53). Kubelka J; Keiderling TA J. Phys. Chem. A 2001, 105, 10922–10928.
(54). Amado AM; Ribeiro-Claro PJA J. Chem. Soc. Faraday T 1997, 93, 2387–2390.
(55). Weidner T; Breen NF; Drobny GP; Castner DG J. Phys. Chem. B 2009, 113, 15423–15426. [PubMed: 19873996]
(56). Zhao X; Ong S; Wang H; Eisenthal KB Chem. Phys. Lett 1993, 214, 203–207.
(57). Garand E; Kamrath MZ; Jordan PA; Wolk AB; Leavitt CM; McCoy AB; Miller SJ; Johnson MA Science, 335, 694–698. [PubMed: 22267579]

(58). Nagornova NS; Rizzo TR; Boyarkin OV Science, 2012, 336, 320–323. [PubMed: 22517854]

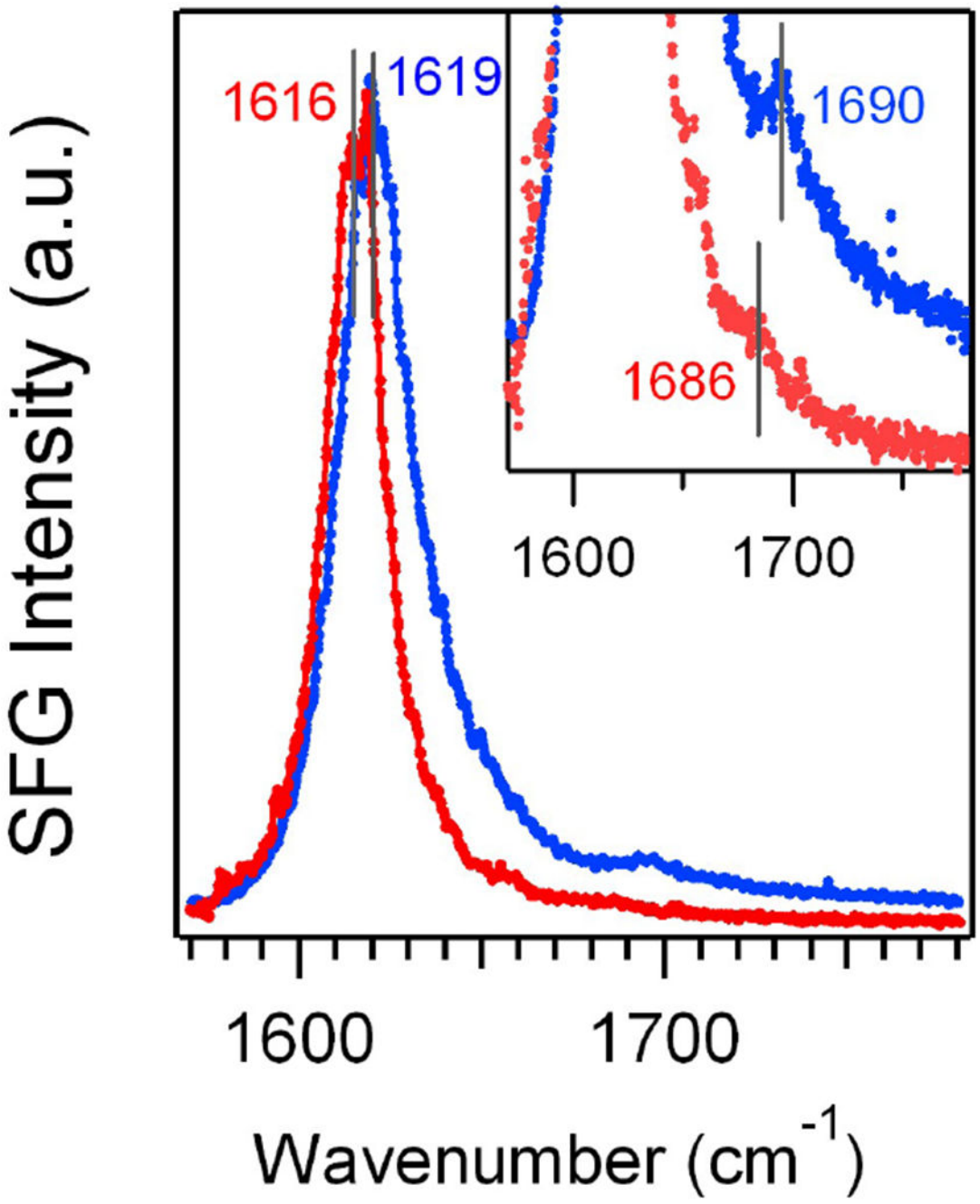

Figure 1.
Chiral amide I spectra of $LK_7\beta$ at the air/H_2O interface (blue) and air/D_2O interface (red).

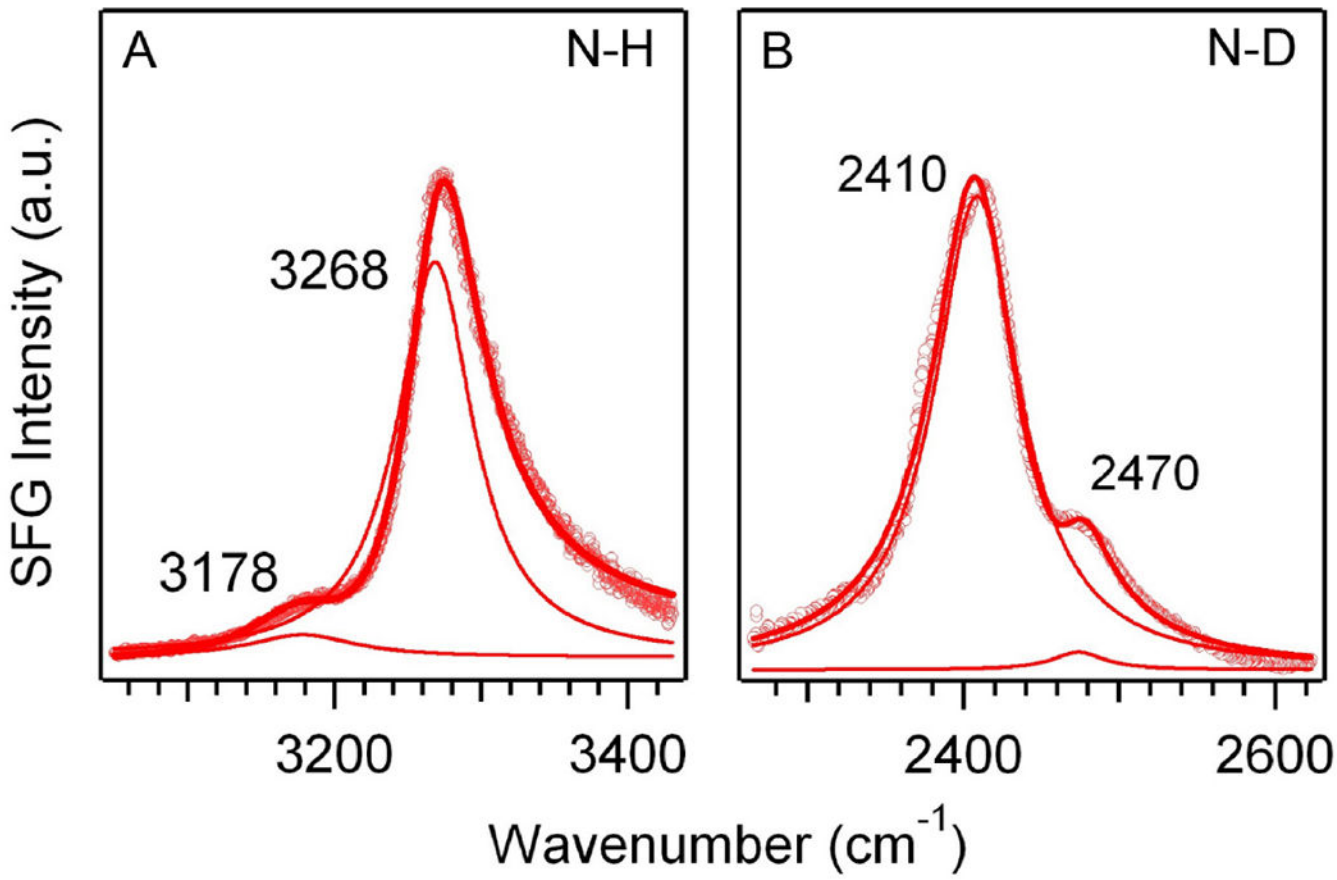

Figure 2.
Chiral SFG spectra of $LK_7\beta$ (A) in the N-H stretch region at the air/H_2O interface and (B) in the N-D stretch region at the air/D_2O interfaces.

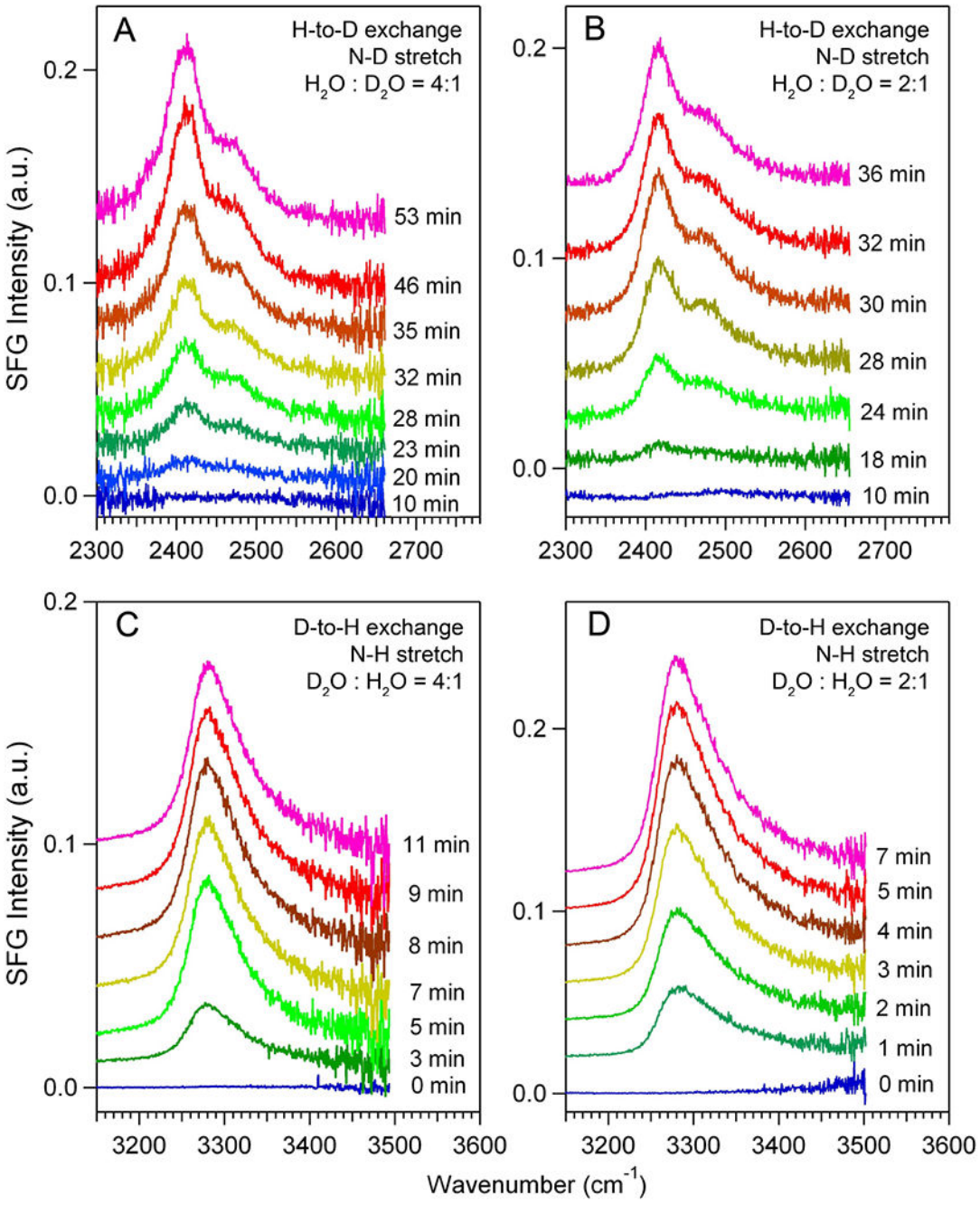

Figure 3.

Kinetics of H/D exchange in $LK_7\beta$ at the air/water interface. Time-dependent N-D stretch spectra of $LK_7\beta$ at the air/ H_2O interface upon addition of D_2O at a ratio of H_2O:D_2O equal to (A) 4:1 and (B) 2:1. Time dependent N-H stretch spectra of $LK_7\beta$ at the air/D_2O interface upon addition of H_2O at a ratio of D_2O:H_2O equal to (C) 4:1 and (D) 2:1.

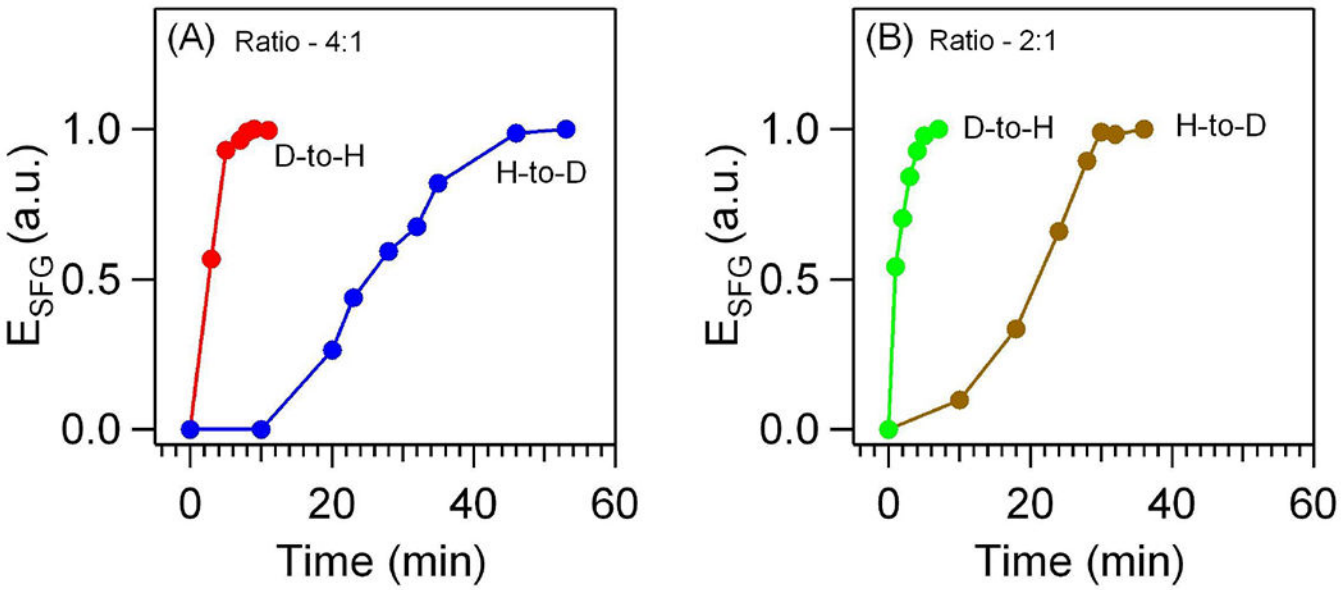

Figure 4.

The time dependence of the SFG field: (A) D-to-H exchange with H_2O:D_2O 4:1 (red) and H-to-D exchange with D_2O:H_2O 4:1 (blue), and (B) D-to-H exchange with D_2O:H_2O 2:1 (green) and H-to-D exchange with H_2O:D_2O 2:1 (brown).

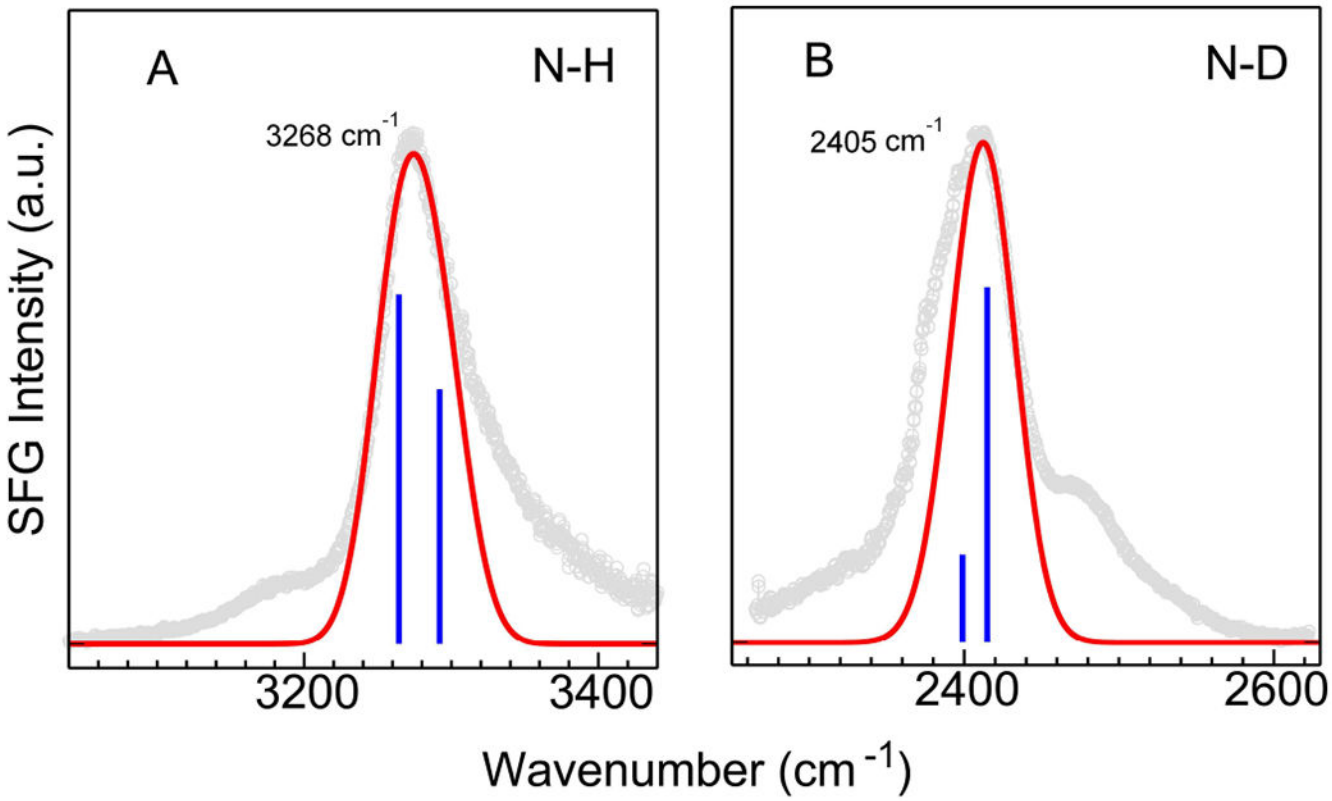

Figure 5.

Calculated *psp* cSFG spectra (*i.e.*, red curves) of non-deuterated and deuterated $LK_7\beta$: (A) N-H stretch region and (B) N-D stretch region, where the grey circles are the experimental spectra, and the blue sticks denote the effective *psp* 2^{nd} susceptibilities squared[44] contributed by individual normal modes. The scaling factor is 0.9322 for the calculated spectra.

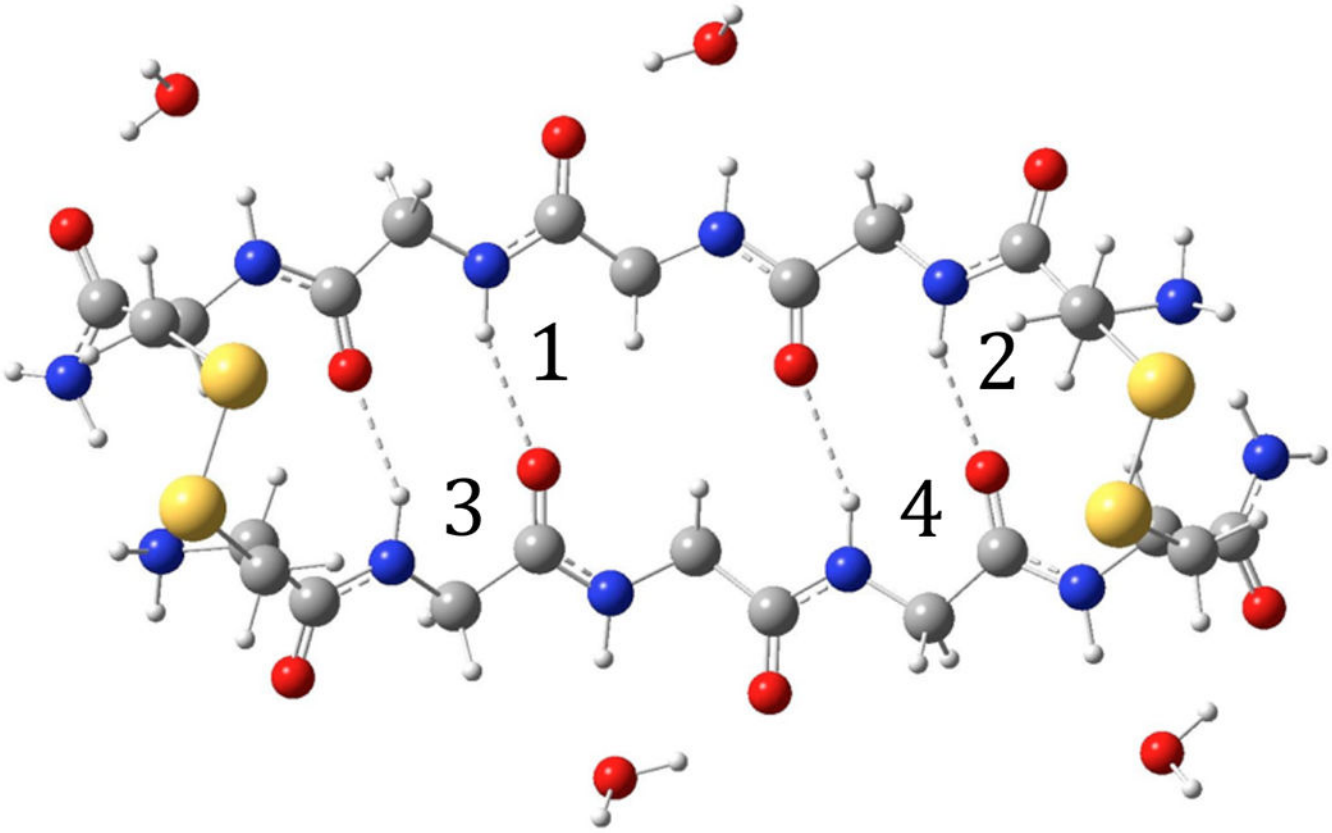

Scheme 1.

An antiparallel β-sheet model consisting of glycine repeat units and two disulfide bonds formed by cysteine residues used for cSFG simulations.

Table 1.

Spectral parameters obtained by fitting the chiral N-H and N-D spectra (Figure 2) into Eq. 1.

Spectra	Fitting parameters	Values
N-H stretch (Figure. 2A)	χ_{NR} (a.u.)	0.154 ± 0.002
	ω_1 (cm^{-1})	3178 ± 0.8
	A_1 (a.u.)	9.6 ± 0.4
	Γ_1 (a.u.)	43.6 ± 1.8
	ω_2 (cm^{-1})	3268 ± 0.1
	A_2 (a.u.)	29.2 ± 0.3
	Γ_2 (a.u.)	31.6 ± 0.2
N-D stretch (Figure. 2B)	χ_{NR} (a.u.)	−0.008 ± 0.002
	ω_1 (cm^{-1})	2473 ± 0.4
	A_1 (a.u.)	2.6 ± 0.2
	Γ_1 (a.u.)	20.2 ± 1.0
	ω_2 (cm^{-1})	2409 ± 0.2
	A_2 (a.u.)	21.9 ± 0.1
	Γ_2 (a.u.)	33.4 ± 0.2

Table 2.

Experimental observed and calculated vibrational frequencies.

Peak Assignment		Exp. (cm^{-1})		Calc. (cm^{-1})	
N-H stretch		3268		3268	
Amide I / *Amide II*	*Combination*	1619 / 1563	3178	1626 / 1545	3171
N-D stretch		2410		2416	
C-N stretch / *N-D bending*	*Combination*	1470 / N/A	2473	1422 / 1044	2466